

DFT/B3LYP Study of the Substituent Effect on the Reaction Enthalpies of the Individual Steps of Single Electron Transfer–Proton Transfer and Sequential Proton Loss Electron Transfer Mechanisms of Phenols Antioxidant Action

Erik Klein* and Vladimír Lukeš

Institute of Physical Chemistry and Chemical Physics, Slovak University of Technology, Radlinského 9, SK-812 37 Bratislava, Slovak Republic

Received: June 5, 2006; In Final Form: September 7, 2006

The reaction enthalpies related to the individual steps of two phenolic antioxidants action mechanisms, single electron transfer–proton transfer (SET-PT) and sequential proton loss electron transfer (SPLET), for 30 meta and para-substituted phenols (ArOH) were calculated using DFT/B3LYP method. These mechanisms represent the alternative ways to the extensively studied hydrogen atom transfer (HAT) mechanism. Except the comparison of calculated reaction enthalpies with available experimental and/or theoretical values, obtained enthalpies were correlated with Hammett constants. We have found that electron-donating substituents induce the rise in the enthalpy of proton dissociation (PDE) from ArOH⁺ radical cation (second step in SET-PT) and in the proton affinities of phenoxide ions ArO[−] (reaction enthalpy of the first step in SPLET). Electron-withdrawing groups cause the increase in the reaction enthalpies of the processes where electron is abstracted, i.e., in the ionization potentials of ArOH (first step in SET-PT) and in the enthalpy of electron transfer from ArO[−] (second step in SPLET). Found results indicate that all dependences of reaction enthalpies on Hammett constants of the substituents are linear. The calculations of liquid-phase reaction enthalpies for several para-substituted phenols indicate that found trends hold also in water, although substituent effects are weaker. From the thermodynamic point of view, entering SPLET mechanism represents the most probable process in water.

Introduction

Phenols are widely used as synthetic organic materials and also as antioxidants in living organisms. Phenoxyl radicals represent important intermediates in many biological and industrial applications.^{1–3} Their importance in relation to the antioxidant activity of phenols has led to an increased interest in these systems in last years. The function of phenolic antioxidants (ArOH) is to intercept and react with free radicals faster than the substrate.^{2,4}

There are two generally accepted mechanisms of phenolic antioxidants action,^{4–6} namely hydrogen atom transfer (HAT) and single-electron transfer followed by proton transfer (SET-PT). The role of the antioxidant is to interrupt the chain reaction according to

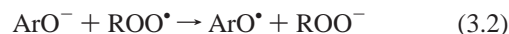


A high rate of hydrogen atom transfer is expected to be related to a low phenolic O–H bond dissociation enthalpy (BDE). Knowledge of the BDEs has been accumulated substantially for the past 15 years, owing to the recent development of both experimental^{3,7–15} and quantum chemical techniques.^{16–28} The second possible mechanism, by which an antioxidant can deactivate a free radical, is single-electron transfer, in which the radical cation ArOH⁺ is first formed, followed by its deprotonation



The net result is the same as in the HAT mechanism (eq 1). Although BDE can be considered the main parameter in HAT, ionization potential (IP) and O–H proton dissociation enthalpy (PDE)^{5,29,30} describe the energetics of the SET-PT process. However, low IP values also enhance the chance of generating a superoxide anion radical through the transfer of the electron directly to surrounding O₂.^{4,31,32}

Recently, another mechanism has been discovered. This was named sequential proton loss electron transfer (SPLET).^{6,33–36} It was experimentally confirmed that vitamin E and other phenols can react with dpph[•] (2,2-diphenyl-1-picrylhydrazil radical) and other electron deficient radicals (ROO[•]) by two different and nonexclusive mechanisms, HAT and SPLET.⁶ SPLET is not uncommon for ArOH/ dpph[•] reactions in solvents that support ionization.³⁶ SPLET can be described by these equations



The reaction enthalpy of the SPLET first step corresponds to the proton affinity, PA, of the phenoxide anion (ArO[−]).^{23,37–39}

* To whom correspondence should be addressed. E-mail: erik.klein@stuba.sk; Phone: ++421 2 59 32 55 35; Fax: ++421 2 52 49 31 98.

In the second step, electron transfer from phenoxide anion to ROO[•] occurs and the phenoxy radical is formed. The reaction enthalpy of this step we will denote as electron transfer enthalpy, ETE. Again, from the antioxidant action viewpoint, the net result of SPLET is the same as in the two previously mentioned mechanisms, i.e., ArOH → ArO[•] + H[•].

Because in chemistry one often needs to compare a group of reactions differing only in the substitution, it is important to study also the effect of substituents on the reaction enthalpy. Substituent effects are among the most important concepts of structural effects influencing the chemical, physicochemical, and biochemical properties of chemical species.^{40,41} In previous work, we have studied various para- and meta-substituted phenols. Molecules and their radical structures were studied using DFT/B3LYP method to calculate the O–H bond dissociation enthalpies (BDEs). Besides, vertical ionization potential (IP_v) values were calculated using DFT/B3LYP and HF methods.^{42,43} Obtained DFT/B3LYP BDEs and HF vertical IPs were found to be in very good accordance with available experimental data. Employed methods describe the effect of substituents on BDE and IP_v satisfactorily, and the results showed that dependences of BDEs and IPs on Hammett constants of the studied substituents were linear.

The goal of this work is to calculate “reaction” IPs (corresponding to the reaction enthalpy of ArOH → ArOH^{•+} + e⁻ process, further denoted as IP_r), PDEs, PAs, and ETEs of phenol and 30 meta- and para-substituted phenols and to assess the substituent effect on these quantities. Except for the comparison of found DFT/B3LYP values with available experimental and/or calculated data, the values of individual quantities will be correlated with Hammett constants published in ref 41. Although in the literature it is possible to find several reports focused on the substituted phenols PDE^{5,30} and PA^{23,37} calculations, these papers do not cover the entire energetics of SET-PT and SPLET mechanisms. Besides, we decided to study a slightly larger set of substituents located in para and meta positions. Except the gas-phase reaction enthalpies, we will compute enthalpies in liquid-phase in water solutions for several para-substituted phenols.

Computational Details. All calculations were performed using the Gaussian 03 program package.⁴⁴ The geometry of each compound, radical, radical cation, and anion was optimized using DFT method with UB3LYP functional without any constraints (energy cutoff of 10⁻⁵ kJ mol⁻¹, final RMS energy gradient under 0.01 kJ mol⁻¹ Å⁻¹). The calculations were performed in the 6-311++G** basis set.⁴⁵ The optimized structures were confirmed to be real minima by frequency calculation (no imaginary frequency). For the species having more conformers, all conformers were investigated. The conformer with the lowest electronic energy was used in this work.

Accuracy of the energy evaluation for systems involving open-shell species is sensitive to spin contamination. Spin contaminations of radicals and radical cations were found in the 0.76–0.78 range. After the annihilation of the first spin contaminant, they dropped to the correct value of 0.75. Therefore, spin contamination should not bias obtained values.

Results and Discussion

In the case of DFT method, which does not provide enthalpies directly, the total enthalpies of the species X, H(X), at the temperature *T* are usually estimated from the expression^{4,5,23,29}

$$H(X) = E_0 + \text{ZPE} + \Delta H_{\text{trans}} + \Delta H_{\text{rot}} + \Delta H_{\text{vib}} + RT \quad (4)$$

where *E*₀ is the calculated total electronic energy, ZPE stands for zero-point energy, Δ*H*_{trans}, Δ*H*_{rot}, and Δ*H*_{vib} are the translational, rotational, and vibrational contributions to the enthalpy, respectively. Finally, *RT* represents PV-work term and is added to convert the energy to enthalpy. Δ*H*_{trans} (3/2 *RT*), Δ*H*_{rot} (3/2 *RT* or *RT* for a linear molecule), and Δ*H*_{vib} contributions to the enthalpy can be calculated from standard formulas.⁴⁶ The zero-point energies can be scaled to reflect the difference between the (harmonic) computed frequencies and the actual anharmonic experimental frequencies^{4,5,29} In this work, the total enthalpies were calculated according eq 4 (*T* = 300 K), and ZPE values were not scaled.

From the calculated total enthalpies, we have determined following quantities

$$\text{IP}_r = H(\text{ArOH}^{\bullet+}) + H(e^-) - H(\text{ArOH}) \quad (5)$$

$$\text{PDE} = H(\text{ArO}^{\bullet}) + H(\text{H}^+) - H(\text{ArOH}^{\bullet+}) \quad (6)$$

$$\text{PA} = H(\text{ArO}^-) + H(\text{H}^+) - H(\text{ArOH}) \quad (7)$$

$$\text{ETE} = H(\text{ArO}^{\bullet}) + H(e^-) - H(\text{ArO}^-) \quad (8)$$

The calculated enthalpy of proton, *H*(H⁺), is 6.197 kJ mol⁻¹; the enthalpy of electron, *H*(e⁻), is 3.145 kJ mol⁻¹.⁴⁷

Ionization Potentials and their Dependence on Hammett Constants. Ionization potentials calculated according eq 5 (IP_r values) are different from those obtained using Koopman's theorem, where vertical IP_v is related directly to the energy of the highest occupied orbital (IP_v = -ε_{HOMO}). IP_r values reflect the geometry relaxation in the radical cation formation process, whereas vertical IPs are related to the neutral molecule geometry. IP_v values, that we calculated using HF method,⁴³ and IP_r values obtained from eq 5 are summarized in the Table 1. We decided to use HF method results instead of DFT data, because DFT significantly underestimates experimentally determined vertical IPs.⁴³ From the comparison of IP_v and IP_r it follows that vertical values are higher by 47–122 kJ mol⁻¹. The largest differences, 100 and 122 kJ mol⁻¹, were found for NMe₂ group in meta and para positions. The average deviation between IP_v and IP_r is 68 kJ mol⁻¹ (0.70 eV). If we exclude data for NMe₂ group, average deviation reaches 65 kJ mol⁻¹.

ΔIP_r values representing the difference between substituted and nonsubstituted phenol IPs, IP(X-PhOH) – IP(PhOH), are summarized in the Table 2. Obtained values show that substituent induced changes in IP_r values are in 233 kJ mol⁻¹ range. Electron-donating substituents lower IP_r values, whereas electron-withdrawing groups cause the increase in the ionization potential. An exceptionally large drop in IP_r induces a strong electron-donating NMe₂ group. Studied substituents induce similar changes in vertical IPs, where calculated values are in 202 kJ mol⁻¹ range.

The Hammett equation (and its extended forms) has been one of the most widely used means for the study and interpretation of organic reactions and their mechanisms. Hammett constants σ_m (for substituent in meta position) and σ_p (for substituent in para position) obtained from ionization of organic acids in solutions can frequently successfully predict equilibrium and rate constants for a variety of families of reactions.⁴¹ Figure 1 shows the correlation between Hammett constants (σ_p and σ_m, shortly denoted as σ_{p,m}) and IP_r values. The equations obtained from the linear regression are as follows

$$\text{IP}_r/\text{kJ mol}^{-1} = 770 + 128\sigma_p \quad (9)$$

$$\text{IP}_r/\text{kJ mol}^{-1} = 756 + 176\sigma_m \quad (10)$$

TABLE 1: Calculated Vertical (IP_v) and Reaction (IP_r) Ionization Potentials and Proton Dissociation Enthalpies (PDE) in kJ Mol^{-1}

substituent	IP_v^a	IP_r	PDE
–	853	806	861
<i>p</i> -NMe ₂	767	645	982
<i>p</i> -NH ₂	763	685	943
<i>p</i> -OH	810	748	898
<i>p</i> -MeO	796	726	918
<i>p</i> - <i>t</i> -Bu	820	759	901
<i>p</i> -Me	822	770	888
<i>m</i> -NH ₂	772	719	943
<i>m</i> -NMe ₂	779	678	986
<i>m</i> - <i>t</i> -Bu	834	772	892
<i>m</i> -Me	841	788	880
<i>p</i> -Ph	790	726	932
<i>p</i> -F	868	808	853
<i>m</i> -Ph	818	751	916
<i>m</i> -OH	847	782	884
<i>m</i> -MeO	831	757	905
<i>p</i> -Cl	862	798	865
<i>p</i> -Br	858	792	872
<i>m</i> -F	892	831	841
<i>m</i> -Cl	886	822	849
<i>m</i> -MeCO	880	817	852
<i>m</i> -Br	884	816	854
<i>m</i> -CF ₃	908	853	824
<i>p</i> -MeCO	889	817	857
<i>p</i> -CF ₃	926	855	824
<i>m</i> -CN	924	862	815
<i>m</i> -MeSO ₂	922	847	828
<i>p</i> -CN	917	851	824
<i>m</i> -NO ₂	940	874	805
<i>p</i> -MeSO ₂	946	852	830
<i>p</i> -NO ₂	965	879	806

^a From ref 43.

Correlation coefficients are 0.957 and 0.910 for the substituents in para and meta positions, respectively. Analogous results we obtain from $\Delta IP_r = f(\sigma_p)$ and $\Delta IP_r = f(\sigma_m)$ correlations, only the line intercept will be lower by 806 kJ mol^{-1} (IP_r of the phenol). Found dependences show that increase in IP_r with Hammett constant is significantly steeper for groups in meta position (the ratio of the line slopes is 1.38).

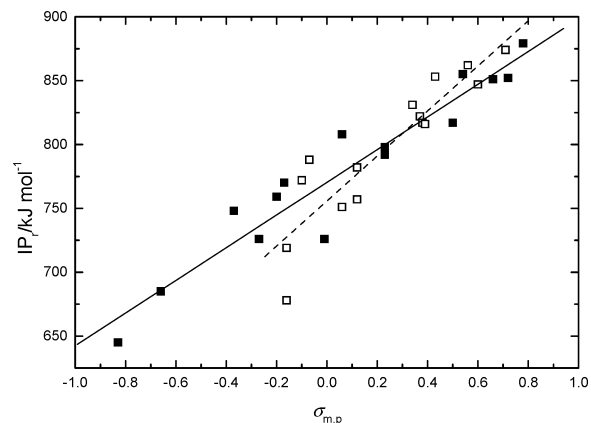
The conversion of IP_r values from kJ mol^{-1} to eV enables us to compare obtained Hammett dependences with those for vertical IPs.⁴³ The comparison of line slopes confirms that both ionization potentials show identical dependence on the Hammett constants. It can be concluded that studied substituents in meta and para positions induce the same change in IP_r and IP_v values.

PDEs and their Dependence on Hammett Constants. PDE represents the reaction enthalpy of the second step in SET-PT mechanism (eq 2.2). For the whole SET-PT mechanism energetics knowledge it is also important to study PDE and the effect of substituents on it. Two theoretical studies of para- and meta-substituted phenol PDEs are available. Zhang et al.³⁰ studied 13 para- and 9 meta-substituted phenols using DFT/B3LYP method with 6-31G** basis set to calculate relative PDEs, i.e., $\text{PDE}(\text{PhOH}) - \text{PDE}(\text{X-PhOH})$ differences. Vafiadis and Bakalbassis⁵ employed DFT/B3LYP method with 6-31+G-(,3pd) basis set to obtain ΔPDEs , where $\Delta\text{PDE} = \text{PDE}(\text{X-PhOH}) - \text{PDE}(\text{PhOH})$, for 13 substituents in para and meta positions. PDEs that we have calculated are shown in Table 1. Table 2 summarizes determined ΔPDEs together with the values published in the two above-mentioned works.^{5,30} Relative PDEs from ref 30 were converted to ΔPDEs ; this resulted only in the change of the sign.

We will focus on the ΔPDE values which can be compared with literature data. From the comparison of the values compiled

TABLE 2: ΔIP_r and ΔPDE Values in kJ mol^{-1} , Hammett Constants $\sigma_{p,m}$ and σ_p^-

substituent	ΔIP_r	ΔPDE			$\sigma_{m,p}^c$	$\sigma_p^-^c$
		6-311++G**	6-31+G(,3pd) ^a	6-31G** ^b		
<i>p</i> -NMe ₂	-161	121	125	121	-0.83	-0.12
<i>p</i> -NH ₂	-121	83	88	91	-0.66	-0.15
<i>p</i> -OH	-58	37	32	42	-0.37	-0.37
<i>p</i> -MeO	-80	57	57	60	-0.27	-0.26
<i>p</i> - <i>t</i> -Bu	-47	40			-0.20	-0.13
<i>p</i> -Me	-37	28	28	26	-0.17	-0.17
<i>m</i> -NH ₂	-87	83	87	85	-0.16	
<i>m</i> -NMe ₂	-128	125	131	122	-0.16	
<i>m</i> - <i>t</i> -Bu	-35	31			-0.10	
<i>m</i> -Me	-18	19	21	20	-0.07	
<i>p</i> -Ph	-81	71			-0.01	0.02
<i>p</i> -F	1	-8	-19	-2	0.06	-0.03
<i>m</i> -Ph	-55	55			0.06	
<i>m</i> -OH	-25	23	20		0.12	
<i>m</i> -MeO	-49	44	46	48	0.12	
<i>p</i> -Cl	-8	4	-5	2	0.23	0.19
<i>p</i> -Br	-14	11	7		0.23	0.25
<i>m</i> -F	24	-20	-28	-16	0.34	
<i>m</i> -Cl	16	-12	-17	-15	0.37	
<i>m</i> -MeCO	11	-9			0.38	
<i>m</i> -Br	10	-7	-7		0.39	
<i>m</i> -CF ₃	46	-37	-49	-29	0.43	
<i>p</i> -MeCO	11	-4			0.50	0.84
<i>p</i> -CF ₃	49	-37	-52	-30	0.54	0.65
<i>m</i> -CN	56	-45	-43	-47	0.56	
<i>m</i> -MeSO ₂	41	-32			0.60	
<i>p</i> -CN	45	-36	-35	-36	0.66	1.00
<i>p</i> -NO ₂	67	-55	-62	-56	0.71	
<i>p</i> -MeSO ₂	46	-31			0.72	1.13
<i>p</i> -NO ₂	72	-55	-65	-61	0.78	1.27

^a From ref 5, PDE of phenol: 871 kJ mol^{-1} . ^b From ref 30. ^c From ref 41.**Figure 1.** Dependence of IP_r vs. σ_p (■, solid line) and σ_m (□, dashed line).

in Table 2, we can see that all three applied approaches give similar results. Electron-donating substituents cause increase in substituted phenols PDEs, whereas electron-withdrawing groups decrease PDE. We found that ΔPDE values are in 180 kJ mol^{-1} range. Zhang et al.³⁰ found ΔPDEs in 196 kJ mol^{-1} , and Vafiadis and Bakalbassis⁵ obtained values in 183 kJ mol^{-1} range. This indicates that all three employed basis sets predict analogous substituent effect on PDE.

The differences between ΔPDEs obtained using the 6-31G**³⁰ and larger 6-311++G** basis set do not exceed 9 kJ mol^{-1} ; the largest discrepancies can be found for *p*-NH₂, *p*-F, *p*-CF₃, *m*-CF₃, and *p*-NO₂ substituents. Deviations in ΔPDEs of the remaining 14 values are within 6 kJ mol^{-1} . The average deviation reached 3.6 kJ mol^{-1} .

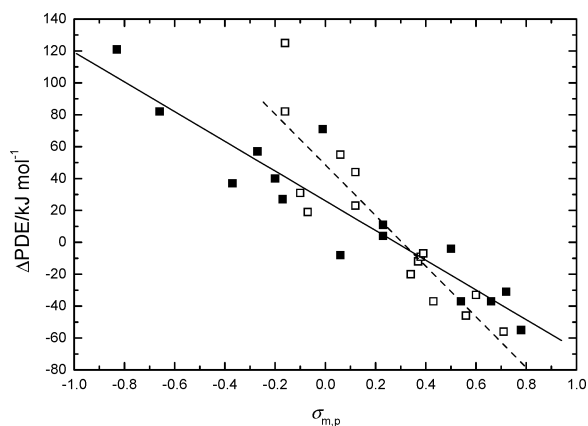


Figure 2. Dependence of ΔPDE vs. σ_p (■, solid line) and σ_m (□, dashed line).

The largest deviations (11–15 kJ mol⁻¹) between our ΔPDE s and those obtained using the 6-31+G(,3pd) basis set⁵ are again predominately for the substituents containing fluorine atom(s), i.e., *p*-F, *p*-CF₃, and *m*-CF₃. The average deviation between the two sets of ΔPDE s reached 5.3 kJ mol⁻¹. If we do not consider *p*-F, *p*-CF₃, and *m*-CF₃ substituents, the average deviation drops to 4.2 kJ mol⁻¹. We can conclude that employed basis sets do not affect ΔPDE s markedly. Substituents containing fluorine atom(s) represent the only exception. A larger difference in ΔPDE was found also for *p*-NO₂ in the case of the 6-311++G** and 6-31+G(,3pd) basis sets.

Studied phenols show roughly linear dependences of ΔPDE s on Hammett constants (Figure 2). These can be described by following equations

$$\Delta\text{PDE}/\text{kJ mol}^{-1} = 26 - 93\sigma_p \quad (11)$$

$$\Delta\text{PDE}/\text{kJ mol}^{-1} = 49 - 159\sigma_m \quad (12)$$

Correlation coefficients reached -0.933 and -0.900. The correlation of ΔPDE s with σ_p^+ constants^{30,40,41} is worse than correlation with σ_p . Zhang et al.⁸ also found better correlation for the groups in the para position, in the case of 9 groups in meta position the correlation coefficient reached only -0.878. Vafiadis and Bakalbassis⁵ obtained similar results, too. The comparison of line slopes indicates that groups in meta position exert stronger influence upon ΔPDE (or PDE) than groups in the para position, i.e., the decrease in PDE with Hammett constant is significantly steeper for groups in meta position (the slopes ratio reached 1.71).

Because in all three possible mechanisms (HAT, SET-PT, and SPLET) the overall result is the same ($\text{ArOH} \rightarrow \text{ArO}^* + \text{H}^*$), ΔBDE represents the sum of ΔIP_r and ΔPDE . In other words, the sum of slopes of $\Delta\text{IP}_r = f(\sigma_{p,m})$ and $\Delta\text{PDE} = f(\sigma_{p,m})$ dependences should correspond to the line slopes of found $\Delta\text{BDE} = f(\sigma_{p,m})$ dependences⁴³

$$\Delta\text{BDE}/\text{kJ mol}^{-1} = -9.8 + 36.7\sigma_p \quad (13)$$

$$\Delta\text{BDE}/\text{kJ mol}^{-1} = -2.01 + 18.7\sigma_m \quad (14)$$

The sums of line slopes for para- and meta-substituted phenols reached 35 and 17, respectively. These are in good agreement with the slopes in eqs 13 and 14. Although the line slopes related to substituents in meta position in $\Delta\text{IP}_r = f(\sigma_m)$ and $\Delta\text{PDE} = f(\sigma_m)$ dependences are significantly steeper than those related to groups in para position, the overall effect is inverse, i.e., the

TABLE 3: Experimental and Calculated Proton Affinities (PA) and Calculated Electron Transfer Enthalpies (ETE) in kJ mol⁻¹

substituent	PA _{ICR} ^a	PA _{HPMS} ^b	PA _{TF} ^c	PA _{LB} ^d	PA	ETE
-	1461	1450	1456	1454	1449	218
<i>p</i> -NMe ₂	1470		1451		1453	174
<i>p</i> -NH ₂	1475	1468	1470	1473	1466	162
<i>p</i> -OH	1470		1462	1463	1455	191
<i>p</i> -MeO	1466	1453	1464	1464	1456	188
<i>p</i> - <i>t</i> -Bu	1458		1454		1449	210
<i>p</i> -Me	1466	1455	1461	1459	1454	204
<i>m</i> -NH ₂	1467	1454		1462	1455	207
<i>m</i> -NMe ₂	1466				1457	207
<i>m</i> - <i>t</i> -Bu	1459				1449	214
<i>m</i> -Me	1463	1452			1452	216
<i>p</i> -Ph					1419	238
<i>p</i> -F	1451	1439	1444	1443	1436	224
<i>m</i> -Ph					1434	233
<i>m</i> -OH	1451	1444		1446	1440	225
<i>m</i> -MeO	1456	1444		1450	1446	216
<i>p</i> -Cl	1436	1422	1433	1427	1422	241
<i>p</i> -Br			1427		1417	247
<i>m</i> -F	1438	1426		1430	1423	248
<i>m</i> -Cl	1431	1417		1420	1415	256
<i>m</i> -MeCO	1433				1415	254
<i>m</i> -Br					1411	260
<i>m</i> -CF ₃	1420			1411	1403	274
<i>p</i> -MeCO	1404				1387	287
<i>p</i> -CF ₃	1410		1402	1399	1390	288
<i>m</i> -CN	1405	1390		1395	1390	288
<i>m</i> -MeSO ₂					1386	289
<i>p</i> -CN	1390		1387	1377	1372	304
<i>m</i> -NO ₂	1399	1376		1391	1383	296
<i>p</i> -MeSO ₂	1385				1371	311
<i>p</i> -NO ₂	1372	1342	1370	1353	1346	339

^a From ref 38. ^b From ref 39. ^c From ref 37. ^d From ref 23.

slope of $\Delta\text{BDE} = f(\sigma_p)$ is steeper than the slope of $\Delta\text{BDE} = f(\sigma_m)$ dependence.

PAs and their Dependence on Hammett Constants. In the case of proton affinities, obtained calculation results can be compared with experimental values. Fujio et al.³⁸ performed gas-phase acidity measurements with pulsed ion cyclotron resonance (ICR) mass spectrometer. Found PAs are shown in the Table 3 (PA_{ICR} column). Standard deviation of the measured values is 8.8 kJ mol⁻¹. McMahon and Kebarle³⁹ determined gas-phase PAs of substituted phenols and benzoic acids; experimental values were measured using pulsed electron beam high-pressure mass spectrometer (HPMS). Their results are summarized in the PA_{HPMS} column of Table 3. Standard deviations of obtained values are in 8–12.5 kJ mol⁻¹ range. The two experimental data sets are in good agreement. Although ICR values are higher than HPMS ones, differences for the majority of substituents do not exceed 15 kJ mol⁻¹ (1%). Larger deviations were found only for *m*-OH, *m*-NO₂, and *p*-NO₂ groups, where differences between determined values are in 22–30 kJ mol⁻¹ range.

Except the experimentally found PAs, calculated values are available, too. Vianello and Maksić³⁷ obtained PAs of para-substituted phenols from MP2(fc)/6-311+G**//B3LYP/6-31G(d) calculations applying triadic formula (TF). Their results are in the column denoted PA_{TF} (Table 3). Chandra and Uchimarū²³ employed the DFT/B3LYP method to compute BDEs and PAs of 9 para- and 9 meta-substituted phenols using two basis sets. Table 3 in the column PA_{LB} contains PAs calculated using the larger, 6-311++G(2df,2p), basis set.²³ Our results for 6-311++G** basis set are summarized in the “PA” column.

From the comparison of obtained PA values with ICR data it is clear, that experimental values are higher, average deviation

TABLE 4: Experimental and Calculated Δ PA Values and Calculated Δ ETE Values in kJ mol^{-1}

substituent	$\Delta\text{PA}_{\text{IRC}}^a$	$\Delta\text{PA}_{\text{HPMS}}^b$	$\Delta\text{PA}_{\text{TF}}^c$	$\Delta\text{PA}_{\text{LB}}^d$	ΔPA	ΔETE
<i>p</i> -NMe ₂	9		-5		4	-44
<i>p</i> -NH ₂	14	18	14	19	18	-56
<i>p</i> -OH	9		6	9	6	-27
<i>p</i> -MeO	5	3	8	10	7	-31
<i>p</i> - <i>t</i> -Bu	-3		-2		1	-8
<i>p</i> -Me	5	5	5	5	5	-14
<i>m</i> -NH ₂	6	4		8	7	-11
<i>m</i> -NMe ₂	5				8	-11
<i>m</i> - <i>t</i> -Bu	-2				0	-4
<i>m</i> -Me	2	2			3	-3
<i>p</i> -Ph					-29	19
<i>p</i> -F	-10	-11	-12	-11	-13	6
<i>m</i> -Ph					-15	15
<i>m</i> -OH	-10	-6		-8	-9	7
<i>m</i> -MeO	-5	-6		-4	-3	-2
<i>p</i> -Cl	-25	-28	-23	-27	-27	23
<i>p</i> -Br			-29		-32	28
<i>m</i> -F	-23	-24		-24	-26	30
<i>m</i> -Cl	-30	-33		-34	-34	38
<i>m</i> -MeCO	-28				-33	35
<i>m</i> -Br					-38	42
<i>m</i> -CF ₃	-41			-43	-46	55
<i>p</i> -MeCO	-57				-62	69
<i>p</i> -CF ₃	-51		-54	-55	-58	70
<i>m</i> -CN	-56	-60		-59	-59	70
<i>m</i> -MeSO ₂					-62	71
<i>p</i> -CN	-71	-74	-69	-77	-77	86
<i>m</i> -NO ₂	-62	-66		-63	-66	78
<i>p</i> -MeSO ₂	-76				-78	93
<i>p</i> -NO ₂	-89	-108	-86	-101	-103	120

^a From ref 38. ^b From ref 39. ^c From ref 37. ^d From ref 23.

is 14.1 kJ mol^{-1} . The largest difference was found in the case of *p*-NO₂ group (26 kJ mol^{-1}). However, the two experimental values are significantly different for this group, too. Our results are in very good agreement with HPMS PAs; the average deviation reached only 2.2 kJ mol^{-1} . Generally, PAs obtained from triadic formula are in better accordance with ICR data, whereas the DFT/B3LYP method gives values closer to HPMS PAs. Applying the larger 6-311++G(2df,2p) basis set²³ results in higher PAs. Differences in the two DFT/B3LYP results are still within the experimental errors range, because the differences between individual values are in $4\text{--}9 \text{ kJ mol}^{-1}$ range and the average deviation reached 6.3 kJ mol^{-1} . We can conclude that our DFT/B3LYP proton affinities are in the best agreement with 16 available HPMS values, whereas the MP2 method (and application of the triadic formula)³⁷ offers values in best accordance with experimental ICR data.³⁸

Table 4 contains ΔPA values; $\Delta\text{PA} = \text{PA}(\text{X-PhOH}) - \text{PA}(\text{PhOH})$. These show that electron-donating substituents slightly increase PA, whereas electron-withdrawing substituents are able to lower PA significantly. Found PAs are in 121 kJ mol^{-1} range. From the ΔPAs point of view, all experimental and calculated values are in considerably good agreement. Larger deviations between the individual data sets can be observed only for the strongest electron-donating and electron-withdrawing groups, *p*-NMe₂ and *p*-NO₂, respectively. Differences between the rest of experimental (ICR, HPMS) and calculated (TF, LB, and our values) ΔPAs exceed 5 kJ mol^{-1} only in three cases. The average deviation between the two experimental data sets is 3.4 kJ mol^{-1} . Deviations between the individual sets of calculated and experimental values lie in $1.9\text{--}5.8 \text{ kJ mol}^{-1}$ range; the largest deviation is between ΔPAs determined from HPMS experiments and the those calculated on the basis of triadic formula.

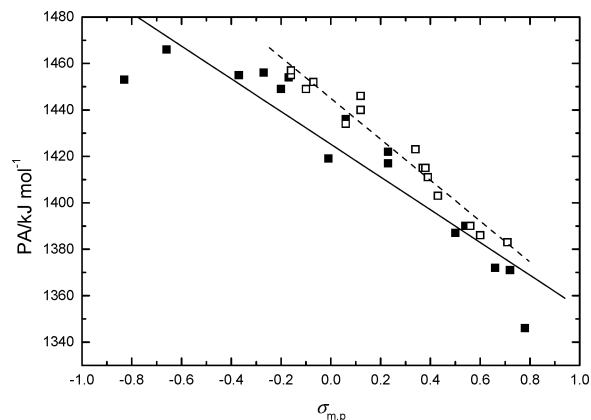


Figure 3. Dependence of PA vs. σ_p (■, solid line) and σ_m (□, dashed line).

Figure 3 shows the $\text{PA} = f(\sigma_p)$ and $\text{PA} = f(\sigma_m)$ dependences. Linear regression provides these equations

$$\text{PA}/\text{kJ mol}^{-1} = 1425 - 71\sigma_p \quad (15)$$

$$\text{PA}/\text{kJ mol}^{-1} = 1445 - 88\sigma_m \quad (16)$$

Correlation coefficients are -0.931 and -0.978 for groups in para and meta positions, respectively. If we exclude *p*-NMe₂ group from the regression analysis, the correlation coefficient reaches -0.965 and the line slope jumps to -82 kJ mol^{-1} . This indicates that substituents located in para and meta positions have rather similar influences on PA. Experimental ICR values follow analogous trends, obtained dependences with correlation coefficients -0.945 (para) and -0.974 (meta) are as follows

$$\text{PA}/\text{kJ mol}^{-1} = 1440 - 66\sigma_p(\text{ICR}) \quad (17)$$

$$\text{PA}/\text{kJ mol}^{-1} = 1457 - 78\sigma_m(\text{ICR}) \quad (18)$$

With the respect to the found standard deviations of the line slopes (6 and 7 kJ mol^{-1} for groups in para and meta positions, respectively), we can conclude that there cannot be observed a significant difference between the two slopes.

In the case of substituents in para position, PA values can be successfully correlated with σ_p^- constants.^{23,37} These are used for phenols and anilines if the permanent negative charge on the reaction site can be resonance stabilized by a substituent.^{23,40} Linear fit confirmed that PA values correlate with σ_p^- constants better in comparison with σ_p constants. We obtained following linear dependence

$$\text{PA}/\text{kJ mol}^{-1} = 1425 - 67\sigma_p^- \quad (19)$$

with the correlation coefficient -0.976 .

ETEs and their Dependence on Hammett Constants.

Electron transfer from the phenoxide ion represents the second step in SPLET mechanism. Although there are no experimental/theoretical values of its reaction enthalpy available, obtained ETEs can be considered reliable, because we found reasonably good agreement between experimental and calculated values of proton affinities and phenolic O–H bond dissociation enthalpies.⁴³ ETE values (Table 3) are significantly lower than PAs. From the calculated data, especially from ΔETEs (Table 4), following trend is observable: electron-donating groups cause the decrease in ETE and electron-withdrawing groups induce the increase in ETE. All values are in the 164 kJ mol^{-1} range. Electron-withdrawing groups alter ETE more than

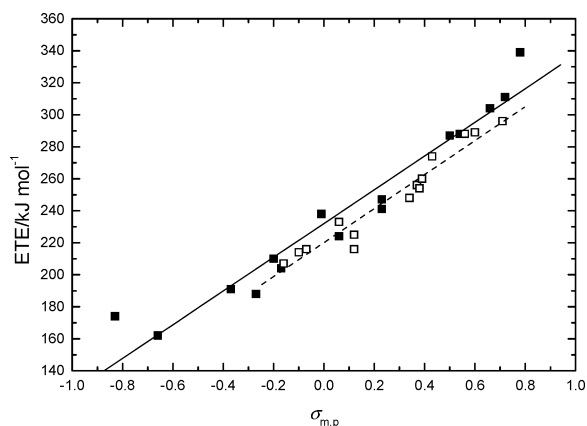


Figure 4. Dependence of ETE vs. σ_p (■, solid line) and σ_m (□, dashed line).

electron-donating ones. Dependences of ETEs on Hammett constants (Figure 4) show that substituents located in para and meta positions exert identical effect upon ETE

$$\text{ETE}/\text{kJ mol}^{-1} = 232.0 + 105.4\sigma_p \quad (20)$$

$$\text{ETE}/\text{kJ mol}^{-1} = 220.1 + 106.3\sigma_m \quad (21)$$

Correlation coefficients reached 0.970 (para) and 0.973 (meta). The sums of the corresponding line slopes of $\text{ETE} = f(\sigma_{p,m})$ and $\text{PA} = f(\sigma_{p,m})$ dependences give 34.4 and 18.3 for para- and meta-substituents, respectively. These values agree with the line slopes describing the substituent effect on BDE (eqs 13 and 14) satisfactorily.

Found Hammett-type dependencies confirm that substituents produce considerable changes in all studied reaction enthalpies. If we compare gas-phase BDEs⁴⁸ and IP_r, we can see that both dependences are analogous. Electron donors cause considerable drop in the two quantities. Electron-withdrawing groups raise BDEs and IP_r values of substituted phenols, however substituent produced changes are smaller. The IP_r/BDE ratios are in 1.82–2.26 range that can be considered narrow. The average IP_r/BDE ratio is 2.12, and 95% of values lie in 2.12 ± 0.04 range. IP_r/BDE ratio rises with the Hammett constants, but this trend is very weak and individual IP_r/BDE values are quite scattered.

From the comparison of BDEs and PAs it is clear that these quantities follow opposite trends. Although electron-donating groups lower BDEs, they cause slight increases in the proton affinities. Electron-withdrawing substituents lower PAs and raise BDEs. The PA/BDE ratio drops from 4.4 (*p*-NMe₂) to 3.4 (*p*-NO₂). PA/BDE ratio decreases with the increase in Hammett constant. The trend can be considered linear because the correlation coefficient of this dependence reached 0.978. Therefore, in comparison to strong electron-donating substituents, we can expect that strong electron-withdrawing groups will have a higher tendency to enter the SPLET reaction pathway.

We can conclude that substituents caused the largest changes in IP_r values. The found ranges of substituent induced changes are in this order: IP_r (233 kJ mol⁻¹) > PDE (180 kJ mol⁻¹) > ETE (164 kJ mol⁻¹) > PA (121 kJ mol⁻¹). These are significantly larger than 62 kJ mol⁻¹ found for BDEs.⁴⁸

Because calculated gas-phase ionization potentials and proton affinities are significantly higher than phenolic O–H group BDEs, we can conclude that homolytic O–H bond splitting-off represents the most probable process in the gas phase from the thermodynamic point of view. Abstraction of the proton from

TABLE 5: Experimental PR and Calculated (PCM model) $\Delta\text{BDE}_{\text{sln}}$ in kJ mol⁻¹

substituent	PR ^a	PCM	$\Delta(\Delta\text{BDE}_{\text{sln}})^b$
<i>p</i> -NH ₂	-53	-56	-3
<i>p</i> -OH	-34	-29	5
<i>p</i> -MeO	-23	-26	-3
<i>p</i> -Me	-9	-10	-1
<i>p</i> -Cl		0	
<i>p</i> -Br		1	
<i>p</i> -MeCO	8	17	9
<i>p</i> -CN	19	21	2
<i>p</i> -NO ₂	25	32	7

^a From ref 10. ^b $\Delta(\Delta\text{BDE}_{\text{sln}}) = \Delta\text{BDE}_{\text{sln}}(\text{PCM}) - \Delta\text{BDE}_{\text{sln}}(\text{PR})$.

the O–H group of a substituted phenol represents the process with the highest energy requirement.

Solvent Effect: Influence of Water on the IP_r, PDE, PA, and ETE. Because SET-PT and SPLET mechanisms are of importance in solvated media, it is interesting to explore how the solvent alters the reaction enthalpies of individual steps of the two mechanisms. To shed light on the solvent effect, we performed PCM (polarized continuum model) method calculations^{22,27,49–51} in B3LYP/6-311++G** basis set for the non-substituted phenol and nine para-substituted phenols in water. PCM method developed by Tomasi and co-workers^{50,51} provides the solvation free energy corresponding to the 1 mol L⁻¹ standard state and 298 K. Although correcting gas-phase enthalpies with PCM solvation free energies does not represent correct approach, calculated enthalpies can be considered reasonable approximations. Moreover, it can be assumed that reaction entropies of the phenolic O–H bond splitting-off are almost identical for the nonsubstituted and substituted phenols⁴⁹ and the contribution stemming from the different standard states related to the gas-phase values and the solvent effect calculations will also cancel in the case of ΔBDE , ΔIP_r , ΔPDE , ΔPA , and ΔETE values. Therefore, these two contributions do not affect the line slopes of the corresponding Hammett dependences. Because Gaussian 03 allows solution-phase geometry optimization, this approach was used for the parent molecules and their respective radicals, radical cations, and anions.

Hereafter, we will label solution related quantities with the subscript “sln”. For the enthalpy of the hydrogen radical, H[•], hydration, we used -4 kJ mol^{-1} value.^{52,53}

BDEs of phenol and para-substituted phenols in the water were calculated to ascertain the reliability of applied computational approach. The obtained phenol BDE_{sln} value, 352 kJ mol⁻¹, is lower than experimentally determined BDE in the water, 369 kJ mol⁻¹.¹⁰ However, 5 kJ mol⁻¹ difference between the calculated gas-phase BDE, 347 kJ mol⁻¹,⁴⁸ and BDE_{sln} is in very good agreement with other published results. Bizzaro et al.,⁵² on the basis of photoacoustic calorimetry experiments and semiempirical AM1 calculation of the difference between enthalpies of hydrated phenol and hydrated phenoxy radical, found that BDE_{sln} of phenol in water is higher than gas-phase BDE by 4 kJ mol⁻¹. The difference between the latest recommended gas-phase BDE (362.4 kJ mol⁻¹)⁵⁴ and the above-mentioned experimental value 369 kJ mol⁻¹ in water is ca. 7 kJ mol⁻¹.

Table 5 contains calculated $\Delta\text{BDE}_{\text{sln}}$ values, where $\Delta\text{BDE}_{\text{sln}} = \text{BDE}_{\text{sln}}(\text{X}-\text{C}_6\text{H}_4\text{OH}) - \text{BDE}_{\text{sln}}(\text{C}_6\text{H}_5\text{OH})$, together with those obtained from pulse radiolysis (PR) experiments¹⁰ for para-substituted phenols in water. It is advantageous to use $\Delta\text{BDE}_{\text{sln}}$ values for the comparison of the substituent effect, because DFT generally underestimates individual BDEs. The differences

TABLE 6: Calculated BDE, IP_r, PDE, PA, and ETE Values of para-Substituted Phenols in Water in kJ mol⁻¹

substituent	BDE _{sln}	IP _{r,sln} ^a	PDE _{sln}	PA _{sln}	ETE _{sln} ^a
–	352	346	6	152	201
<i>p</i> -NH ₂	297	237	60	165	132
<i>p</i> -OH	323	291	32	160	163
<i>p</i> -MeO	326	296	30	157	169
<i>p</i> -Me	342	326	15	156	186
<i>p</i> -Cl	352	347	6	143	236
<i>p</i> -Br	353	345	8	142	211
<i>p</i> -MeCO	369	377	–8	121	247
<i>p</i> -CN	373	394	–22	121	251
<i>p</i> -NO ₂	384	410	–27	102	281

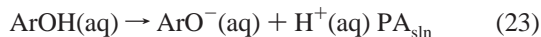
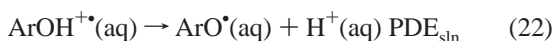
^a Values represent lower limits. For explanation, see the text.

between calculated and experimental $\Delta\text{BDE}_{\text{sln}}$ values did not exceed 9 kJ mol⁻¹. The average deviation between calculated and experimental $\Delta\text{BDE}_{\text{sln}}$ values reached 4.1 kJ mol⁻¹. Such deviations are usual for the results of various experimental approaches, too.^{3,7,9–11}

It is also interesting to compare calculated and experimental BDEs when we want to compare energy requirements of all possible mechanisms of phenols antioxidant action. Obtained BDE_{sln} values are in 297–384 kJ mol⁻¹ range (Table 6), whereas experimental values lie in 316–394 kJ mol⁻¹ range.¹⁰ Differences are in the range from 10 to 19 kJ mol⁻¹ and the average deviation reached 14.9 kJ mol⁻¹.

Calculated $\Delta\text{BDE}_{\text{sln}}$ and BDE_{sln} values show that chosen approach may provide reasonable results for the estimation of substituent effects on the reaction enthalpies related to SET-PT and SPLET mechanisms in water solutions and for the comparison of energy requirements related to HAT, SET-PT, and SPLET mechanisms. We can compare only calculated and experimental BDE_{sln} values, because no experimental study of the energetics of SET-PT and SPLET mechanisms in solvated media is available yet.

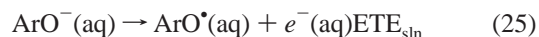
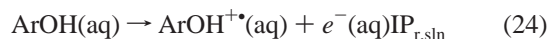
Water causes considerable changes of the enthalpies of molecule, radical, anion and the radical cation of studied phenols. Hydration of nonsubstituted phenol, its radical cation and radical produces 224 kJ mol⁻¹ decrease in IP_r and 235 kJ mol⁻¹ increase in PDE. In the case of SPLET mechanism, hydration of the molecule and anion caused 207 kJ mol⁻¹ drop in PA. On the other hand, obtained ETE is due to hydration of anion and radical higher by 219 kJ mol⁻¹. All these values do not take the enthalpies of H⁺ and electron hydration into account. Enthalpy of H⁺ hydration is –1090 kJ mol⁻¹.⁴⁶ It severely affects the enthalpy of reaction in these two processes



For phenol, it results in PDE_{sln} = 6 kJ mol⁻¹ and PA_{sln} = 152 kJ mol⁻¹.

Because the enthalpy of electron hydration, $\Delta_{\text{hydr}}H(e^-)$, could not be found in the literature, its upper limit was estimated from the calculated gas-phase total enthalpies of proton (6.197 kJ mol⁻¹), electron (3.145 kJ mol⁻¹),⁴⁷ and hydrogen atom (–1312.479 kJ mol⁻¹) and the enthalpies of hydration of the hydrogen atom (–4 kJ mol⁻¹)^{49,50} and H⁺ (–1090 kJ mol⁻¹).⁴⁶ The thermodynamic cycle treatment gives $\Delta_{\text{hydr}}H(e^-) = -236$ kJ mol⁻¹, when the enthalpy of H⁺(aq) + e⁻(aq) → H[•](aq) reaction is zero. Actually, this reaction has to be exothermic and the true $\Delta_{\text{hydr}}H(e^-)$ value has to be higher (less negative).

Because IP_{r,sln} and ETE_{sln}, related to the following reactions



depend on $\Delta_{\text{hydr}}H(e^-)$, using $\Delta_{\text{hydr}}H(e^-) = -236$ kJ mol⁻¹, one can find lower limits of IP_{r,sln} and ETE_{sln}. For the phenol it represents IP_{r,sln} = 346 kJ mol⁻¹ and ETE_{sln} = 201 kJ mol⁻¹. Calculated PA_{sln} and PDE_{sln} values together with estimated lower limits of IP_{r,sln} and ETE_{sln} values are compiled in the Table 6. It can be assumed that actual IP_{r,sln} and ETE_{sln} are by several tens of kJ mol⁻¹ higher. However, $\Delta_{\text{hydr}}H(e^-)$ value does not affect substituent induced changes in IP_{r,sln} and ETE_{sln} values expressed as $\Delta\text{IP}_{\text{r,sln}}$ and $\Delta\text{ETE}_{\text{sln}}$ (differences between the enthalpies of substituted phenol and the phenol itself).

PA_{sln} values from Table 6 indicate that the energy requirement of the SPLET first step in water is significantly lower than BDE_{sln} or IP_{sln}. BDE_{sln} values and lower limits of IP_{r,sln} values for the majority of studied substituents are similar. We can conclude that in water SPLET represents the most probable reaction pathway from the thermodynamic point of view, i.e., low PA_{sln} values favor entering SPLET. PA_{sln} decreases with an increase in the electron-withdrawing effect (Hammett constant) of a substituent. For electron-withdrawing groups, the difference between BDE_{sln} and PA_{sln} values is significantly more pronounced in comparison to strong electron-donating groups. Whereas the BDE_{sln}/PA_{sln} ratio for NH₂ reached 1.8, in the case of the NO₂ group, this ratio is 3.8. This implies that substituted phenols with an electron-withdrawing group may enter the SPLET pathway more likely than phenols with electron-donating substituents.

Using linear regression, for the studied quantities, we have obtained the following dependences on σ_p (or σ_p^-)

$$\text{IP}_r = 325 + 109\sigma_p \quad (26)$$

$$\text{PDE} = 16 - 53\sigma_p \quad (27)$$

$$\text{PA} = 151 - 35\sigma_p^- \quad (28)$$

$$\text{ETE} = 197 + 98\sigma_p \quad (29)$$

Absolute values of the correlation coefficients are in 0.977–0.985 range. All these dependences are less steep than those found for gas-phase data. However, for IP_r and ETE values, the differences are relatively small. Moreover, the regression analysis was performed only for 9 groups instead of all 15. Obtained results predict a smaller effect of substituents on the studied quantities in water. However, found trends remain identical. Generally, Hammett-type dependences play also important prediction role, because obtained equations enable to estimate new IP, PDE, PA, and ETE values from Hammett constants or vice versa.

Understanding why one mechanism is preferred over another requires knowledge of both thermodynamics and kinetics of the reaction. Besides, the kinetic barriers related to individual steps of a considered mechanism are also important. For example, it is known that reactions of C–H bonds and carbon radicals are much (10⁴) slower than analogous reactions of RO–H and RO[•] at the same driving force.⁵⁵ Depending on the solvent and present radical species properties, in the solutions one of the possible antioxidant action mechanisms may prevail, as it was confirmed in refs 33–36. Because HAT does not involve charge separation, it is preferred in nonpolar solvents, whereas SET-PT and SPLET mechanisms are favored in polar media due to

the charge separation process.⁵⁶ Our results show that solvent may affect substituent induced changes in the studied quantities in some extent, although for BDEs and especially for Δ BDEs it was found that solvents/phases and experimental techniques employed to determine BDEs do not affect Δ BDEs markedly.^{3,7,9–11,15,48} On the other hand, DFT/B3LYP calculations showed certain differences between Δ BDE values in a vacuum and in DMSO solutions,²² especially for strong electron-donating groups. However, trends in the substituent effects should be independent of the phase or solvent.

Conclusions

In this article, the reaction enthalpies of the individual steps of two antioxidant action mechanisms, SET-PT and SPLET, for meta- and para-substituted phenols were studied. Both mechanisms may represent alternative ways to the extensively studied HAT mechanism (mainly in terms of BDEs). The calculations provided the full information related to the energy requirements of the two mechanisms. We can conclude that the DFT/B3LYP method with 6-311++G** basis set gives proton dissociation enthalpies and proton affinities in very good agreement with the available experimental and/or theoretical data. Because in all studied mechanisms the overall result is identical with that of HAT mechanism, obtained values of ionization potentials (representing the reaction enthalpy of $X\text{-PhOH} \rightarrow X\text{-PhOH}^{+\bullet} + e^-$) and enthalpies of electron transfer from phenoxide ion can also be considered reliable.

We have found that electron donating substituents induce the rise in PDE and PA, whereas electron-withdrawing groups cause the increase in the reaction enthalpies of the processes where the electron is abstracted (IPs and ETEs). Groups in meta position have in comparison with the substituents in para position significantly greater influence on IP and PDE, i.e., for the groups in para position the same difference in Hammett constant leads to smaller change in these quantities. In the case of the PAs that are related to SPLET mechanism, the same difference in Hammett constant also leads to larger change in PAs for the groups in meta position. However, this difference is not so pronounced as in the case of IPs and PDEs. The two dependences of ETEs on Hammett constants ($\sigma_{p,m}$) have practically identical line slopes; substituents in both positions induce the same change in ETE.

Finally, we have estimated IP_r, PDE, PA, and ETE values of phenol and nine para-substituted phenols in water and confirmed that found trends are valid also for the liquid-phase values. However, the results indicate that solvation attenuates the substituent effect, especially in the case of PDEs and PAs. From the thermodynamic point of view, entering SPLET mechanism represents the most probable process in water.

Acknowledgment. Dedicated to Professor V. Kvasnicka on the occasion of his 65th birthday. This work has been supported by Science and Technology Assistance Agency under the contract No APVT-20-005004. The work has been also supported by Slovak Grant Agency (VEGA 1/2021/05, 1/3566/06).

References and Notes

- Halliwell, B.; Gutteridge, J. M. C. *Free Radicals in Biology and Medicine*, 2nd Ed.; Oxford University Press: Oxford, 1989.
- Gugumus, F. *Oxidation Inhibition in Organic Materials*, Vol. 1; CRC Press: Boca Raton, 1990.
- Zhu, Q.; Zhang, X. M.; Fry, A. J. *Polym. Degrad. Stab.* **1997**, *57*, 43.
- Wright, J. S.; Johnson, E. R.; DiLabio, G. A. *J. Am. Chem. Soc.* **2001**, *123*, 1173.
- Vafiadis, A. P.; Bakalbassis, E. G. *Chem. Phys.* **2005**, *316*, 195.
- Musialik, M.; Litwinienko, G. *Org. Lett.* **2005**, *7*, 4952.
- Denisov, E. T. *Polym. Degrad. Stab.* **1995**, *49*, 71.
- Bordwell, F. G.; Zhang, X.-M.; Satish, A. V.; Cheng, J.-P. *J. Am. Chem. Soc.* **1994**, *116*, 6605.
- Bordwell, F. G.; Cheng, J.-P. *J. Am. Chem. Soc.* **1991**, *113*, 1736.
- Lind, J.; Shen, X.; Eriksen, T. E.; Merenyi, G. *J. Am. Chem. Soc.* **1990**, *112*, 479.
- Mulder, P.; Saastad, O. W.; Griller D. *J. Am. Chem. Soc.* **1988**, *110*, 4090.
- Wayner, D. D. M.; Luszytk, E.; Pagé, D.; Ingold, K. U.; Mulder, P.; Laarhoven, L. J. J.; Aldrich, H. S. *J. Am. Chem. Soc.* **1995**, *117*, 8737.
- Wayner, D. D. M.; Luszytk, E.; Ingold, K. U. *J. Org. Chem.* **1996**, *61*, 6430.
- Correia, C. F.; Nunes, P. M.; dos Santos, R. M. B.; Simões, J. A. M. *Thermochim. Acta* **2004**, *420*, 3.
- de Heer, M. I.; Korth, H.-G.; Mulder, P. *J. Org. Chem.* **1999**, *64*, 6969.
- Pratt, D. A.; DiLabio, G. A.; Mulder, P.; Ingold, K. U. *Acc. Chem. Res.* **2004**, *37*, 334.
- Haerberlein, M.; Brinck, T. *J. Phys. Chem.* **1996**, *100*, 10116.
- Johnson, E. R.; Clarkin, O. J.; DiLabio, G. A. *J. Phys. Chem. A* **2003**, *107*, 9953.
- DiLabio, G. A.; Pratt, D. A.; LoFaro, A. D.; Wright, J. S. *J. Phys. Chem. A* **1999**, *103*, 1653.
- Brinck, T.; Haerberlein, M.; Jonsson, M. *J. Am. Chem. Soc.* **1997**, *119*, 4239.
- Wright, J. S.; Carpenter, D. J.; McKay, D. J.; Ingold, K. U. *J. Am. Chem. Soc.* **1997**, *119*, 4245.
- Fu, Y.; Liu, L.; Mou, Y.; Lin, B.-L.; Guo, Q.-X. *J. Mol. Struct. (THEOCHEM)* **2004**, *674*, 241.
- Chandra, A. K.; Uchimaru, T. *Int. J. Mol. Sci.* **2002**, *3*, 407.
- Yao, X.-Q.; Hou, X.-J.; Jiao, H.; Xiang, H.-W.; Li, Y.-W. *J. Phys. Chem. A* **2004**, *108*, 10834.
- Estácio, S. G.; do Couto, P. C.; Cabral, B. J. C.; da Piedade, M. E. M.; Simões, J. A. M. *J. Phys. Chem. A* **2003**, *107*, 9991.
- Cabral, B. J. C.; Canuto, S. *Chem. Phys. Lett.* **2005**, *406*, 300.
- Bakalbassis, E. G.; Lithoxidou, A. T.; Vafiadis, A. P. *J. Phys. Chem. A* **2003**, *107*, 8594.
- Klein, E.; Matis, M.; Lukeš, V.; Cibulková, Z. *Polym. Degrad. Stab.* **2005**, *91*, 262.
- Zhang, H.-Y.; Ji, H.-F. *J. Mol. Struct. (THEOCHEM)* **2003**, *663*, 167.
- Zhang, H.-Y.; Sun, Y.-M.; Wang, X.-L. *J. Org. Chem.* **2002**, *67*, 2709.
- Pratt, D. A.; DiLabio, G. A.; Brigati, G.; Pedulli, G. F.; Valgimigli, L. *J. Am. Chem. Soc.* **2001**, *123*, 4625.
- Burton, G. W.; Doba, T.; Gabe, E. J.; Hughes, L.; Lee, F. L.; Prasad, L.; Ingold, K. U. *J. Am. Chem. Soc.* **1985**, *107*, 7053.
- Litwinienko, G.; Ingold, K. U. *J. Org. Chem.* **2003**, *68*, 3433.
- Litwinienko, G.; Ingold, K. U. *J. Org. Chem.* **2004**, *69*, 5888.
- Foti, M. C.; Daquino, C.; Geraci, C. *J. Org. Chem.* **2004**, *69*, 2309.
- Litwinienko, G.; Ingold, K. U. *J. Org. Chem.* **2005**, *70*, 8983.
- Vianello, R.; Maksić, Z. B. *Tetrahedron* **2006**, *62*, 3402.
- Fujio, M.; McIver, R. T.; Taft, R. W. *J. Am. Chem. Soc.* **1981**, *103*, 4017.
- McMahon, T. B.; Kebarle, P. *J. Am. Chem. Soc.* **1977**, *99*, 2222.
- Krygowski, T. M.; Stępień, B. T. *Chem. Rev.* **2005**, *105*, 3482.
- Hansch, C.; Leo, A.; Taft, R. W. *Chem. Rev.* **1991**, *91*, 165.
- Klein, E.; Lukeš, V.; Cibulková, Z.; Polovková, J. *J. Mol. Struct. (THEOCHEM)* **2006**, *758*, 149.
- Klein, E.; Lukeš, V. *Chem. Phys.* submitted.
- Frisch, M. J.; Trucks, G. W.; Schlegel, H. B.; Scuseria, G. E.; Robb, M. A.; Cheeseman, J. R.; Montgomery, J. A., Jr.; Vreven, T.; Kudin, K. N.; Burant, J. C.; Millam, J. M.; Iyengar, S. S.; Tomasi, J.; Barone, V.; Mennucci, B.; Cossi, M.; Scalmani, G.; Rega, N.; Petersson, G. A.; Nakatsuji, H.; Hada, M.; Ehara, M.; Toyota, K.; Fukuda, R.; Hasegawa, J.; Ishida, M.; Nakajima, T.; Honda, Y.; Kitao, O.; Nakai, H.; Klene, M.; Li, X.; Knox, J. E.; Hratchian, H. P.; Cross, J. B.; Bakken, V.; Adamo, C.; Jaramillo, J.; Gomperts, R.; Stratmann, R. E.; Yazyev, O.; Austin, A. J.; Cammi, R.; Pomelli, C.; Ochterski, J. W.; Ayala, P. Y.; Morokuma, K.; Voth, G. A.; Salvador, P.; Dannenberg, J. J.; Zakrzewski, V. G.; Dapprich, S.; Daniels, A. D.; Strain, M. C.; Farkas, O.; Malick, D. K.; Rabuck, A. D.; Raghavachari, K.; Foresman, J. B.; Ortiz, J. V.; Cui, Q.; Baboul, A. G.; Clifford, S.; Cioslowski, J.; Stefanov, B. B.; Liu, G.; Liashenko, A.; Piskorz, P.; Komaromi, I.; Martin, R. L.; Fox, D. J.; Keith, T.; Al-Laham, M. A.; Peng, C. Y.; Nanayakkara, A.; Challacombe, M.; Gill, P. M. W.; Johnson, B.; Chen, W.; Wong, M. W.; Gonzalez, C.; Pople, J. A. *Gaussian 03*, revision A.1; Gaussian, Inc.: Pittsburgh, PA, **2003**.
- Binkley, J. S.; Pople, J. A.; Hehre W. J. *J. Am. Chem. Soc.* **1980**, *102*, 939.

- (46) Atkins P. W. *Physical Chemistry*, 6th ed.; Oxford University Press: Oxford, 1998.
- (47) Bartmess, J. E. *J. Phys. Chem.* **1994**, 98, 6420.
- (48) Klein, E.; Lukes, V. *J. Mol. Struct. (THEOCHEM)* **2006**, 767, 43.
- (49) Fu, Y.; Liu, L.; Guo, Q.-X. *J. Phys. Org. Chem.* **2004**, 17, 282.
- (50) Tomasi, J.; Persico, M. *Chem. Rev.* **1994**, 94, 2037.
- (51) Barone, V.; Cossi, M.; Tomasi, J. *J. Chem. Phys.* **1997**, 107, 3210.
- (52) Bizarro, M. M.; Cabral, B. J. C.; dos Santos, R. M. B.; Simões, J. A. M. *Pure Appl. Chem.* **1999**, 71, 1249.
- (53) Parker, W. D. *J. Am. Chem. Soc.* **1992**, 114, 7458.
- (54) Mulder, P.; Korth, H.-G.; Pratt, D. A.; DiLabio, G. A.; Valgimigli, L.; Pedulli, G. F.; Ingold, K. U. *J. Phys. Chem. A* **2005**, 109, 2647.
- (55) Mayer, J. M.; Rhile, I. J. *Biochim. Biophys. Acta* **2004**, 1655, 51.
- (56) Zhang, H.-Y.; Ji, H.-F. *New J. Chem.* **2006**, 30, 503.